COMPARING 1st-, 2nd - AND 3rd-GENERATION COASTAL WAVE MODELLING

L.H. Holthuijsen[1], N. Booij[1] and IJ.G. Haagsma[1]

ABSTRACT

The SWAN wave model for shallow water is used in three generation modes to show the differences in results between these modes and with observations in two real, rather field situations. These are situations of waves approaching two different sites in the Netherlands and Germany: one closed part of an estuary and one region between and beyond barrier islands with channels and tidal flats. The differences between the modes are significant (more than 25% locally) in terms of significant wave height and mean wave period. These differences are ascribed, at least partially to the indirect effects of triad wave-wave interactions which shorten the wave period. The observations are located at positions where the differences between the modes are hardly significant.

INTRODUCTION

Over the last decade, the traditional wave ray models to compute waves in coastal regions are being replaced by models that compute the waves on a regular grid. In analogy with ocean wave models, three generations of such grid models can be distinguished. The differences between these generations are essentially in the approximation of the physical processes, in particular in the representation of the nonlinear wave-wave interactions. Here we compare computational results of all three generations against each other and against observations in two real, rather complex field cases.

THE WAVE MODEL

In the present study the three modes of the spectral wave model SWAN of Booij et al. (1996) are used. The 1st- and 2nd-generation mode are essentially those of the DOLPHIN model of Holthuijsen and de Boer (1988; see also Holthuijsen et al., 1993) in which wave generation and dissipation are formulated with fairly simple expressions. In the 3rd-generation mode all processes are represented explicitly as in the WAM Cycle 3 model (WAMDI group, 1988), supplemented with depth-induced wave breaking and triad

[1]) Delft University of Technology, Department of Civil Engineering and Geosciences, Stevinweg 1, 2628 CN Delft, the Netherlands

wave-wave interactions. The formulations of these three modes that are used in the present study are briefly described next without the effects of currents.

Basic equation

In the absence of ambient currents, the basic equation of SWAN is the discrete spectral energy balance which can be written as (e.g. Hasselmann et al., 1973):

$$\frac{\partial}{\partial t}E + \frac{\partial}{\partial x}c_x E + \frac{\partial}{\partial y}c_y E + \frac{\partial}{\partial \theta}c_\theta E + \frac{\partial}{\partial \sigma}c_\sigma E = S$$

where E is the energy density as function of intrinsic frequency, spectral direction, spatial coordinates and time $E=E(\sigma,\theta;x,y,t)$. The first term in the left-hand side of this equation represents the local rate of change of energy density, the second and third term represent wave propagation in geographical space. The fourth term represents propagation is the spectral domain (refraction and frequency shifting due to (time) variations in depth). The expressions for the propagation speeds in these terms are taken from linear wave theory. The term S $(=S(\sigma,\theta;x,y,t))$ at the right hand side of the action balance equation is the source term representing the effects of generation, dissipation and nonlinear wave-wave interactions (to be addressed below).

Generation

Transfer of wind energy to the waves is described in SWAN with a resonance mechanism (linear growth in time) and a feed-back mechanism (exponential growth). In the 1st- and 2nd-generation mode of this model, the expression for the linear growth is due to Cavaleri and Malanotte-Rizzoli (1981). In the 3rd-generation mode it is ignored. In all three generation modes the expression for the exponential growth is due to Snyder et al. (1981) with different coefficients in the three modes: for the 1st- and 2nd-generation mode they have been obtained from fitting results to standard, fetch-limited deep water growth curves and for the 3rd-generation mode they are taken from WAM Cycle 3.

Dissipation

The formulations for bottom friction and depth-induced wave breaking are the same for all three modes of SWAN. Bottom friction is represented with the JONSWAP expression of Hasselmann et al. (1973) with the bottom friction coefficient of Bouws and Komen (1983). Depth-induced wave breaking has been modelled with a spectral version of the random-bore model of Battjes and Janssen (1978) that retains the shape of the spectrum during breaking. The remaining dissipation due to whitecapping is simulated in 1st- and 2nd-generation mode by terminating the wave growth per spectral component when an upper limit in energy density is achieved. This upper limit is a shallow-water version of the Pierson-Moskowitz (PM) spectrum formulated in terms of wave number and with a $\cos^2(\theta - \theta_{wind})$ directional distribution. Its peak frequency is taken from the SPM (1973; with deep water obviously as a special case). The energy scale coefficient α of this limit spectrum is an increasing function of decreasing depth that is tuned to standard shallow-water growth curves (it has the conventional value of $\alpha = 0.0081$ in deep water). If the energy density is larger than this limit spectrum (e.g. due to a change in wind speed or direction), whitecapping is simulated with a relaxation model with a frequency-dependent time scale that is small for high frequencies and very long for low frequencies. In 3rd-

generation mode, the whitecapping formulation is based on the pulse-based model of Hasselmann (1974), as adapted by the WAMDI group (1988) for the WAM model.

Nonlinear wave-wave interactions

The effects of quadruplet wave-wave interactions on wave growth in 1st- and 2nd-generation mode is simulated by enhancing the above described wind input term with a factor five. In 2nd-generation mode, the overshoot effect of these interactions is additionally simulated: the energy scale parameter α of the assumed limit spectrum is taken to be a decreasing function (obtained by tuning to standard deep-water growth curves) of the dimensionless energy of the wind sea part of the spectrum. The actual spectrum thus obtained with 1st- and 2nd-generation mode in standard, deep-water, fetch-limited situations is very similar to the JONSWAP spectrum, slowly changing into the PM spectrum with $\alpha = 0.0081$ for the fully developed situation. In 3rd-generation mode the quadruplet interactions are computed explicitly with the Discrete Interaction Approximation (DIA) of Hasselmann et al. (1985).

Triad wave-wave interactions are computed explicitly only in 3rd-generation mode with the Lumped Triad Approximation (LTA) of Eldeberky (1996).

APPLICATIONS

The three modes of modelling are applied to two real field cases in the Netherlands with complex bathymetry, 95% reduction in the observed wave energy due to depth-induced wave breaking with subsequent local generation by wind. These cases will first be shown here with the results of the 3rd-generation mode of SWAN. In the next section the results of the other modes will be addressed in terms of differences with these 3rd-generation results.

Haringvliet

The Haringvliet is a branch of the Rhine estuary in the south-west of the Netherlands that is separated from the main estuary by sluices. The bathymetry of the area and the locations of the (eight) observation stations are shown in Fig. 1. A local storm generated on October 14, 1982 waves from north-westerly directions and the SWAN computations are carried out for 23:00 UTC on this day. The incident wave conditions and the wind are given in Table 1 (significant wave height H_s and the mean wave period $\overline{T}$ defined as $H_s = 4\sqrt{m_0}$ and $\overline{T} = 2\pi (m_1 / m_0)$ where $m_m = \int \sigma^n E(\sigma,\theta))$. Figures 2 and 3 show the 3rd-generation results for the significant wave height and the mean wave period The waves approach the estuary from deep water and break over a shoal with a reduction of significant wave height from about 3.6 m in deep water to 2.5 m just in front of the shoal to about 0.6 m just behind the shoal. The local wind regenerates the waves behind the shoal to about 1.1 m significant wave height at station 8.

Norderneyer Seegat

The Norderneyer Seegat (Fig. 4) is a tidal gap between the barrier islands of Juist and Norderney in the northern part of Germany. The region behind this gap is an inter-tidal area with shoals and channels over a distance of 7.5 km to the main land. A high-tide case (November 17, 1995, 04:00 UTC) has been selected (no currents, Table 1). Figures 5 and 6 show the computed pattern of the significant wave and mean wave period. As the

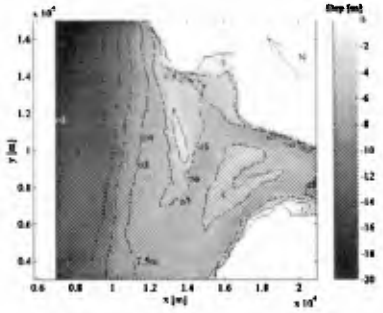

Fig. 1 The bathymetry of the Haringvliet with the eight observation stations.

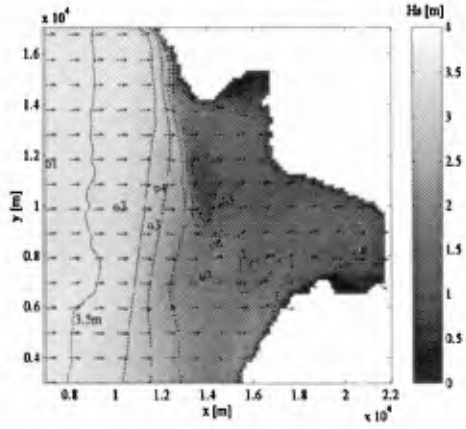

Fig. 2 The computed pattern (3rd-generation) of the significant wave height and mean wave direction (unit vectors; Haringvliet)

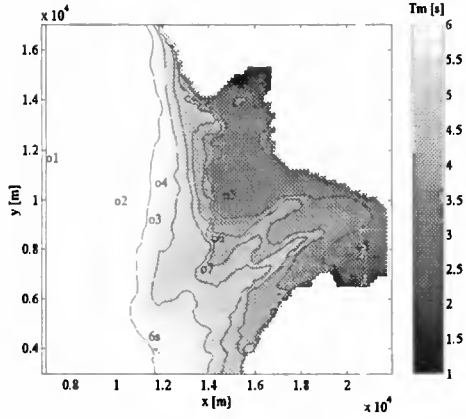

Fig. 3 The computed pattern (3rd-generation) of the mean wave period (Haringvliet).

	$H_{s,i}$ (m)	$\overline{T}$ (s)	$\overline{\theta}_{wave,i}$ (°)	$\sigma_{\theta,i}$ (°)	U_{10} (ms^{-1})	θ_{wind} (°)
Haringvliet	3.56	6.7	306	31	14	300
Norderneyer Seegat	2.98	6.8	375	45	8	338

Table 1 The incident significant wave height, mean wave period, mean wave direction, directional spreading and wind speed and direction for the two cases of this study.

waves propagate from deep water to the barrier islands the wave height gradually decreases from about 3 m to about 2.5 m at station 2. As the waves propagate through the gap they refract out of the channels to the shallower parts where wave energy is dissipated rapidly and local wind regenerates high-frequency waves.

MODEL INTERCOMPARISON

The results of the 1st- and 2nd-generation modes are qualitatively very similar to those of the 3rd-generation mode shown above. Therefore only the differences will be shown. These are presented as relative differences, defined as $\Delta H_s = [\, H_{s,3} - H_{s,i} \,] / H_{s,3}$ and $\Delta \overline{T} = [\, \overline{T}_3 - \overline{T}_i \,] / \overline{T}_3$ where the subscript $_3$ refers to the 3rd-generation results and the subscript $_i$ to either the 1st-generation or 2nd-generation results. The differences for the Haringvliet for the 1st-generation mode are given in Fig. 7 where it is obvious that the differences are relatively large over and behind the shoal, north of the shoal and in the sheltered area deep in the bay (south of station 8). Beyond the shoal the significant wave height is typically 15% lower in the 1st-generation results than in the 3rd-generation results and the mean wave period is some 20% longer (50% over the shoal). In the 2nd-generation results the differences are qualitatively very similar but they are quantitatively considerably smaller, as shown in Fig. 8. The differences in significant wave height in the areas lateral of the shoal (seen in the direction of wave propagation) seem to be due to differences in refraction (not shown here). These in turn seem to be induced by the differences in mean wave period up-wave from these locations (to be addressed later). The differences in the sheltered area south of station 8 may well be due to differences in short-fetch wave growth.

For the Norderneyer Seegat, the differences for 1st-generation mode are given in Fig. 9. Again it is obvious that the differences are relatively large, particularly in the channels and in the short-fetch areas behind the islands. The differences for 2nd-generation mode are again qualitatively equal to those in 1st-generation mode but quantitatively smaller as shown in Fig. 10. As in the Haringvliet case, the differences seem to be related to differences in refraction (due to differences in period) and short-fetch wave growth.

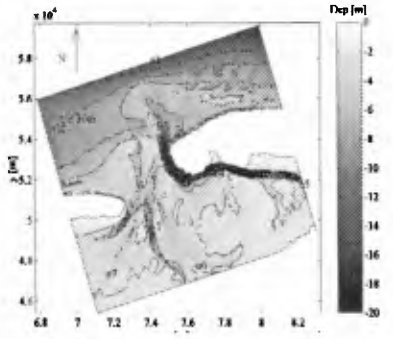

Fig. 4 The bathymetry of the Norderneyer Seegat with the locations of nine observation stations.

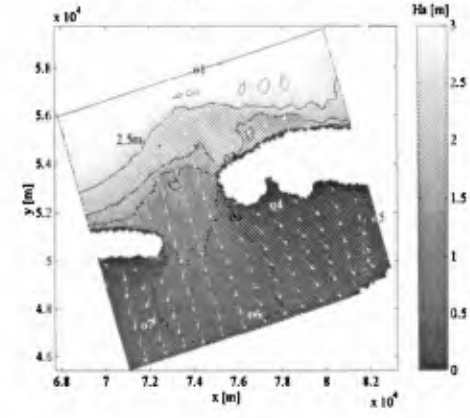

Fig. 5 The computed pattern of the significant wave height and mean wave direction (unit vectors; Norderneyer Seegat).

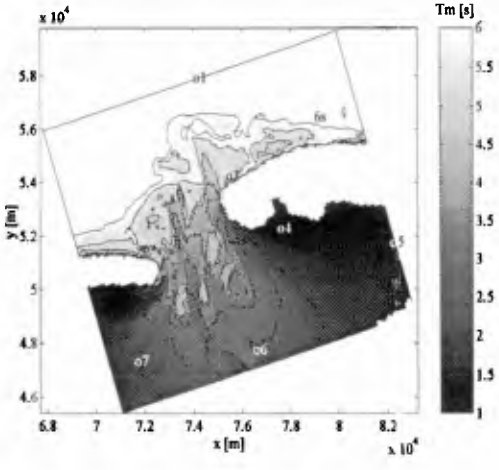

Fig. 6 The computed pattern of the mean wave period (Norderneyer Seegat).

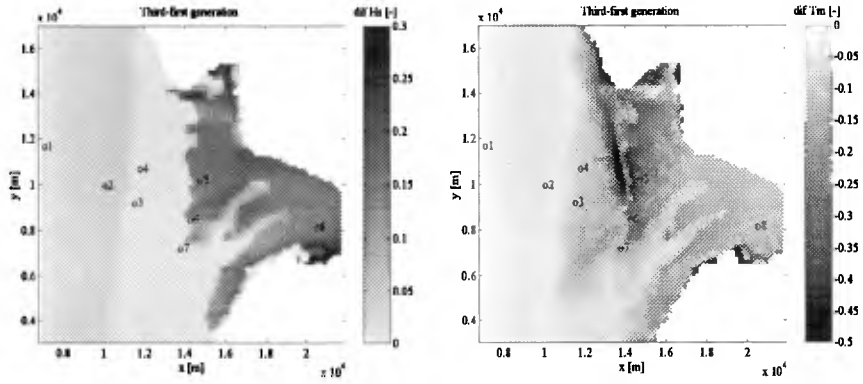

Fig. 7 The relative differences in significant wave height and mean wave period for the Haringvliet (1st-generation compared to 3rd-generation).

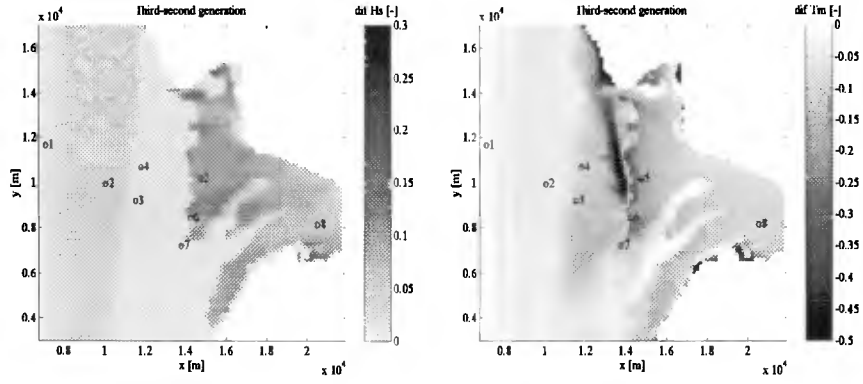

Fig. 8 The relative differences in significant wave height and mean wave period for the Haringvliet (2nd-generation compared to 3rd-generation).

DISCUSSION

The above differences are attributed (partly) to differences in refraction which in turn would be due to differences in wave periods due to the absence of triad wave-wave interactions in the 1st-generation and 2nd-generation mode. This is inferred from the stronger refraction in 1st-generation and 2nd-generation results than in the 3rd-generation results (not shown). The computations were therefore repeated for the Norderneyer Seegat

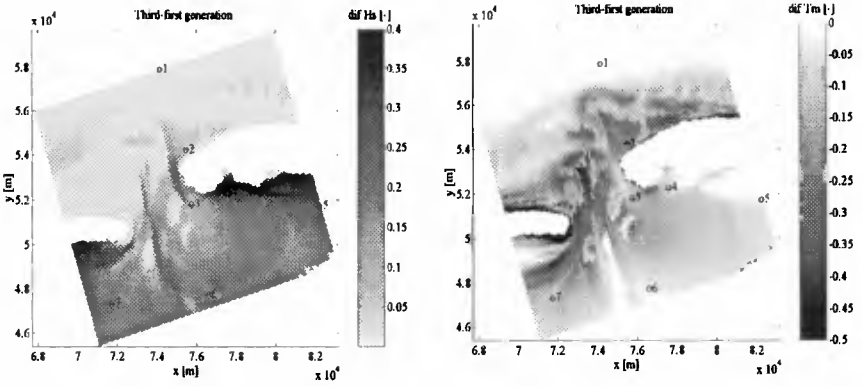

Fig. 9 The relative differences in significant wave height and mean wave period for the Norderneyer Seegat (1st-generation compared to 3rd-generation).

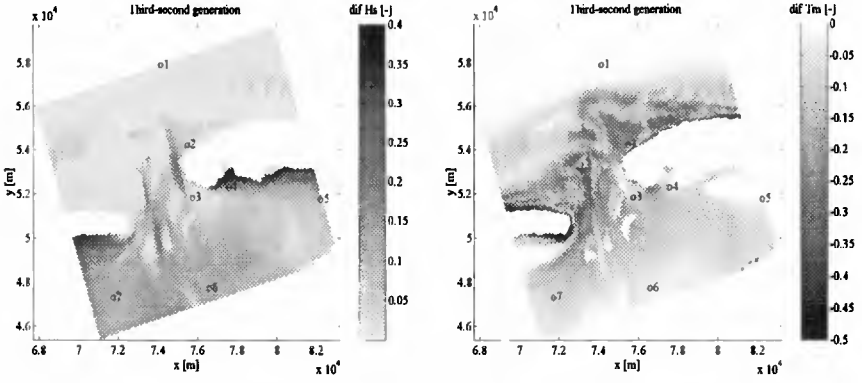

Fig. 10 The relative differences in significant wave height and mean wave period for the Norderneyer Seegat (2nd-generation compared to 3rd-generation).

where the refraction effect seems to be particularly clear, with the 3rd-generation mode without triad wave-wave interactions. These results seem to confirm that indeed refraction is affected by these interactions (through the difference in wave periods). To show that other effects can be ignored, these computations have been repeated without refraction (by de-activating the refraction term in the basic equation). The results are shown in Fig. 11 and they confirm the speculation about the indirect effect of the triad wave-wave interactions on refraction.

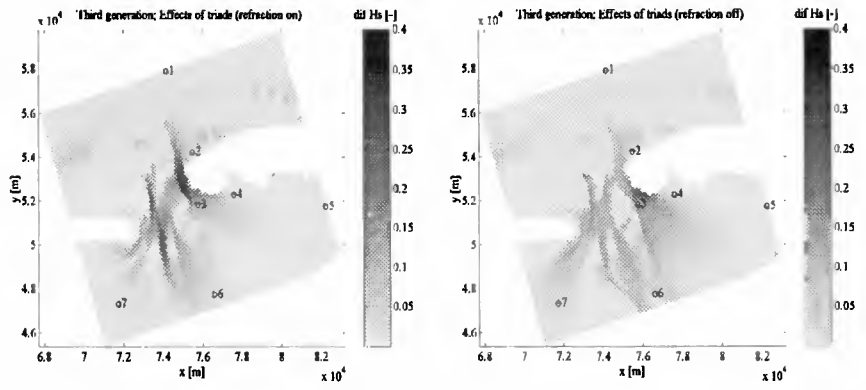

Fig. 11 The effect of triad wave-wave interactions on the refraction in the Norderneyer Seegat. Left panel: relative difference in significant wave height in 3rd generation mode due to disabling refraction with triad wave-wave interactions active, right panel: relative difference in significant wave height due to disabling refraction in 3rd generation mode without triad wave-wave interactions.

	Haringvliet		Norderneyer Seegat	
	rms H_s (m)	rms $\overline{T}$ (s)	rms H_s (m)	rms $\overline{T}$ (s)
1st-generation	0.33	0.45	0.23	0.84
2nd-generation	0.33	0.28	0.24	0.88
3rd-generation	0.39	0.43	0.23	1.03

Table 2 The root-mean-square errors (model results *vs* observations) for the 1st-, 2rd and 3rd-generation mode for the Haringvliet and Nordeneyer Seegat cases of this study.

The observations (see Figs. 3 and 6 for locations) should tell which of the three modes of SWAN provide the best wave estimates. Unfortunately, most of the observations have been taken in regions where the differences between the three modes are rather small (less than 10%). This is also obvious from the small differences between the errors in the three modes (see Table 2).

CONCLUSIONS

In the rather complex coastal field conditions of this study, the triad wave-wave interactions in the SWAN model (3rd-generation mode) generate a shorter wave period in very shallow water than in either the 1st- or 2nd-generation mode of SWAN. This affects the refraction pattern of the waves wich in turn affects the pattern of significant wave height. Moreover, the short-fetch wave growth is very different between the three modes.

Although a fair amount of observations is available, the locations of these observations are not well suited to discriminate between the three modes.

ACKNOWLEDGEMENTS

We are very grateful to John de Ronde, Joska Andorka Gal and their co-workers at the Ministry of Transport, Public Works and Water Management (the Netherlands) for providing us with the data of the Haringvliet. We are equally indebted to Hanz Niemeyer and Ralf Kaiser of the Niedersächsisches Landesamt für Ökologie - Forschungsstelle Küste - (Germany) for providing us with the data of the Norderneyer Seegat.

REFERENCES

Battjes, J.A. and J.P.F.M. Janssen, 1978: Energy loss and set-up due to breaking of random waves, *Proc. 16th Int. Conf. Coastal Engineering*, ASCE, 569-587

Booij, N., L.H. Holthuijsen and R.C. Ris, 1996, The "SWAN" wave model for shallow water, *Proc. 25th Int. Conf. Coastal Engineering*, 668-676

Bouws, E. and G.J. Komen, 1983: On the balance between growth and dissipation in an extreme, depth-limited wind-sea in the southern North Sea, *J. Phys. Oceanogr.*, **13**, 1653-1658

Cavaleri, L. and P. Malanotte-Rizzoli, 1981: Wind wave prediction in shallow water: Theory and applications. *J. Geophys. Res.*, **86**, No. C11, 10,961-10,973

Eldeberky, Y., 1996: Nonlinear transformation of wave spectra in the nearshore zone, Ph.D. thesis, Delft University of Technology, The Netherlands, 203 p.

Hasselmann, K., et al., 1973: Measurements of wind-wave growth and swell decay during the Joint North Sea Wave Project (JONSWAP), *Dtsch. Hydrogr. Z. Suppl.*, **12**, A8

Hasselmann, K., 1974: On the spectral dissipation of ocean waves due to whitecapping, *Bound.-layer Meteor.*, **6**, 1-2, 107-127

Hasselmann, S., K. Hasselmann, J.H. Allender and T.P. Barnett, 1985: Computations and parameterizations of the linear energy transfer in a gravity wave spectrum. Part II: Parameterizations of the nonlinear transfer for application in wave models, *J. Phys. Oceanogr.*, **15**, 11, 1378-139

Holthuijsen, L.H. and S. De Boer, 1988: Wave forecasting for moving and stationary targets, *Computer modelling in Ocean Engineering*, Eds. B.Y. Schrefler and O.C. Zienkiewicz, Balkema, Rotterdam, The Netherlands, 231-234

Holthuijsen, L.H., N. Booij and L. Bertotti, 1993, The effect of wind errors on ocean wave hindcasts, In: Proc. 12th Int. Conf. OMAE, ASME, Vol. 2, pp. 117-124

Snyder, R.L., Dobson, F.W., Elliott, J.A. and R.B. Long, 1981: Array measurement of atmospheric pressure fluctuations above surface gravity waves, *J. Fluid Mech.*, **102**, 1-59

SPM, Shore Protection Manual, 1973, U.S. Army Coastal Eng. Res. Center, Corps of Engineers, 1145 p.

WAMDI group, 1988: The WAM model - a third generation ocean wave prediction model, *J. Phys. Oceanogr.*, **18**, 1775-1810